Int. J. Electrochem. Sci., 8 **(2013)** 9201 - 9221

International Journal of
ELECTROCHEMICAL
SCIENCE
www.electrochemsci.org

Adenine as an Effective Corrosion Inhibitor for Stainless Steel in Chloride Solution

Mieczyslaw Scendo[*], *Joanna Trela*

Institute of Chemistry, Jan Kochanowski University in Kielce, Swietokrzyska 15G, PL– 25406 Kielce, Poland
[*]E-mail: scendo@ujk.edu.pl

Received: 24 April 2013 / *Accepted:* 2 June 2013 / *Published:* 1 July 2013

The influence of the concentration of adenine (AD) on the corrosion of 304 austenic stainless steel in chloride acid solutions was studied. The investigations involved electrochemical polarization methods, scanning electron microscopy (SEM) and quantum chemical calculations method. Tafel polarization study revealed that AD acted as a mixed-type inhibitor. The inhibition efficiency increased with an increase in the concentration of adenine. The adsorption of AD has been found to occur on the surface of 304 austenic stainless steel according to the Langmuir isotherm. The kinetic and thermodynamic parameters for stainless steel corrosion and adenine adsorption, respectively were determined and discussed.

Keywords: A. Austenic stainless steel; A. Adenine; B. Tafel polarization; C. Kinetic parameters; C. Thermodynamic parameters

1. INTRODUCTION

The anticorrosive properties of the stainless steel materials which a chromium contained higher than 12% are assigned to the spontaneous formation on the surface of a passive thin film layer, mainly composed of chromium and iron oxides/hydroxides [1]. The rate of corrosion of stainless steel can be reduced by a thin oxide layer formed naturally on the metal surface [2]. Passive films on surface of stainless steel formed in an aqueous acid environment are usually very thin, compact and highly enriched in chromium [3-5]. Despite the established corrosion resistance of stainless steel can be chemically attacked by acids, and some organic compounds. The passive surface layer of the steel is eroded by these acids resulting in corrosion of the stainless steel.

Corrosion inhibitors are needed to reduce the corrosion rates of metallic materials in this area. Many *N*-heterocyclic compounds, and their derivatives such as: triazole [6,7], tetrazole [8], pyridine [9-11], pyrazole [12,13], pyrimidine [14], pyridazine [15], indole [16,17], and quinoline [18] have been investigated in destination of use they as inhibitors of corrosion of different species of steels.

Most of the inhibitors are toxic in nature, therefore, their replacement by environmentally benign inhibitors is necessary. These compounds include such amino acids and its derivatives as mimosa, tannin or isatin which have been tested in acid solutions for various metals [19-23].

As an important *N*-heterocyclic compound, purine (PU) and purine derivatives are nontoxic and biodegradable, what makes the investigation of their inhibiting properties significant in the context of the current priority to produce eco-friendly inhibitors. Recently, purine and adenine (AD) have been studied as corrosion inhibitors of copper in aggressive solutions [24-27]. However, appeared that purine considerably slows down corrosion of stainless steel [28].

The industrial consumption and development of new corrosion inhibitors have been continuously increasing of the years.

The present work reported the inhibitive effect concentration of adenine (AD) and temperature on the corrosion of 304 austenic stainless steel in 1.1 M chloride acid solutions.

1.1. Adenine structure

Adenine is relatively cheap and easy to produce in purity greater than >99%. The non-toxic and biodegradable nature of adenine makes the investigation of its inhibiting properties significant in the context of the current priority to produce *green* or *environmentally friendly* inhibitors.

The distribution of charge densities for the AD molecules was calculated by PM3 semi-empirical methods using a HyperChem® v. 7.5 software. The structure of AD is given in Figure 1.

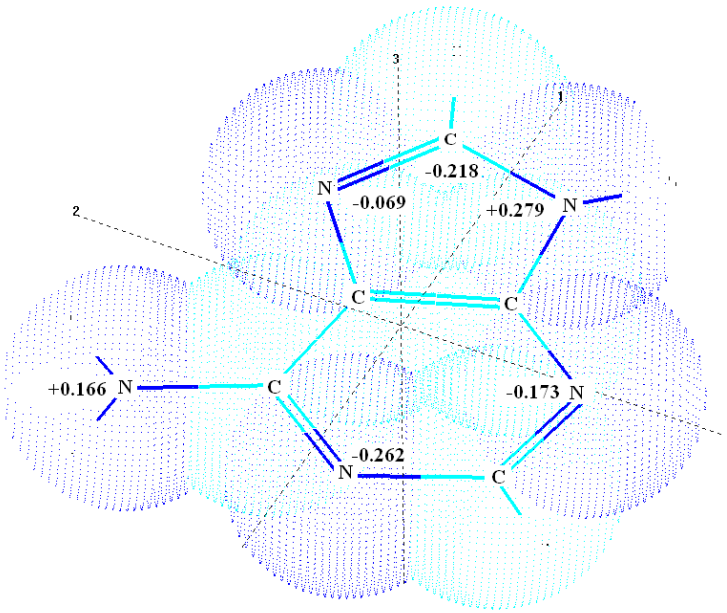

Figure 1. Molecular structure of adenine (AD) obtained after a geometric optimization procedure

Adenine molecules are of small size and have ideal plane structure which can make the electronic effects more important and the steric effects omitted. Adenine possesses weak basic proprieties. The constants protonation/deprotonation have values pK_{a1} = 4.25 and pK_{a2} = 9.83. Unfortunately, still does not establish to which nitrogen atoms in molecule of adenine proton attaches [29].

2. EXPERIMENTAL

2.1. Solutions

Adenine, $C_5H_5N_5$ (> 99.4%) was purchased from Merck (Darmstadt, Germany). The electrolytes were prepared using analytical grade reagents (Merck). The corrosive medium was prepared from a stock NaCl and 1.0 M HCl solution. Adenine was dissolved at concentrations in the range of 0.1 - 10 mM in 1.1 M Cl^- acid solutions (pH 1.5). All solutions were prepared from double distilled water. For each experiment a freshly made solution was used. All test have been performed in naturally aerated electrolytes.

2.2. Electrodes and apparatus

Experiments were carried out in a three-electrode glass cell with a 200 cm^3 capacity. The testing material was austenitic type 304 (X5CrNi18/10 according to PN-EN 10088) stainless steel. The steel composition was as follows (in wt.%): C: 0.07, Cr: 18.0, Ni: 9.0, Mn: 2.0, Si: 0.8, P: 0.045, S: 0.03 and Fe: balance. The working electrode was prepared in the shape of rectangle which had a surface area of 4.62 cm^2. Prior to each experiment, the working electrode surface was treated with 800, 1200, and 2000 grade emery paper to give a mirror like surface finish, and then thoroughly rinsed with double distilled water. After this the electrode was degreased with ethanol in an ultrasonic bath (~5 min) and then rinsed with double distilled water. The electrode was taken immersed in the test electrolyte.

Electrode potentials were measured and reported against the external saturated calomel electrode (SCE) connected to the cell via a Luggin probe. The capillary tip was opposite to the end of the working electrode and about 3 mm from it.

A platinum wire was used as an auxiliary electrode. Reference and auxiliary electrodes were individually isolated from the test solution by glass frits.

All voltammetric experiments were performed using a potentiostat/galvanostat PGSTAT 128N, AutoLab, Netherlands with NOVA 1.7 software the same firm.

The values reported in the paper represent mean values of at least three replicate measurements. Moreover, all experiments were carried out at suitably well-chosen temperature (±0.5 ^{0}C) in an air thermostat with the forced air circulation.

2.3. Potentiodynamic experiments

The electrochemical behaviour of stainless steel sample in uninhibited and inhibited solution was studied by recording potentiodynamic polarization curves. The electrode potential from -700 to 0 mV vs. SCE at a scan rate of 1 mV s^{-1}. The linear Tafel segments of cathodic and anodic curves were extrapolated to corrosion potential (E_{corr}) to obtain corrosion current densities (j_{corr}).

The polarization resistance (R_p) were evaluated from the measured j_{corr} values using the relationship [30,31]:

$$R_p = \frac{B}{j_{corr}} \quad (1)$$

where B is constant which was obtained by following equation:

$$B = \frac{b_c\, b_a}{2.303\,(b_c + b_a)} \quad (1a)$$

Moreover, the degree of surface coverage, and the corrosion inhibition efficiency were calculated from the equations:

$$\Theta = 1 - \frac{j_{corr}}{j^0_{corr}} \quad (2)$$

and:

$$IE(\%) = \frac{j^0_{corr} - j_{corr}}{j^0_{corr}} \times 100 \quad (3)$$

where j_{corr} is the corrosion current density at a particular adenine concentration, and j^0_{corr} is the corrosion current density in the absence of inhibitor in the solution.

All the recorded j_{corr} values are converted into the corrosion rate (υ_p) using the expression:

$$\nu_p\left(mm\ y^{-1}\right) = 3280\times10^{-3}\ \frac{j_{corr}\ M}{n\ \rho} \quad (4)$$

where b_c, b_a are the Tafel slopes, M is the molar mass of iron, n is the number of electrons transferred in the corrosion reaction, and ρ is the density of iron.

2.4. Quantum chemical calculation

HyperChem 7.5 a quantum–mechanical program Hypercube Inc (Gainesville, Florida, USA) was used for molecular modeling. The calculation was based on semi-empirical PM3 method with 3-21G* basis set. Quantum chemical parameters such as the highest occupied molecular orbital (HOMO) the lowest unoccupied molecular orbital (LUMO) energy gap ($\Delta E = E_{LUMO} - E_{HOMO}$) and dipole moment ($\mu$) were calculated.

2.5. Scanning electron microscopy

The morphology of the corrosion products formed on the surface of 304 austenic stainless steel in 1.1 M Cl^- solution in absence and presence of 10 mM of adenine for 360 hours were tested by scanning electron microscope (SEM) JSM-5400 with beam energies in the 0.2 – 20 kV range.

3. RESULTS AND DISCUSION

3.1. Potentiodynamic polarization measurements

The potentiodynamic polarization measurements were carried out in order to gain knowledge concerning the kinetics of the cathodic and anodic reactions.

3.1.1. Non-inhibited solutions

The electrochemical behaviour of 304 austenic stainless steel sample in non-inhibited solutions which contained: 1.1, 0.55, and 0.275 M Cl^- were studied. The pH of solutions were changed in range 1.5 – 2. The potentiodynamic polarization curves are presented in Figure 2.

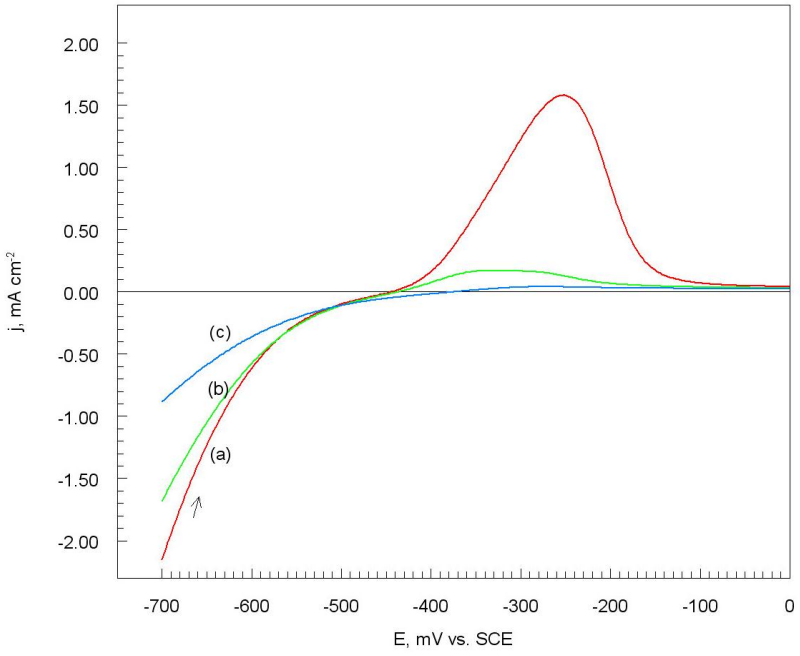

Figure 2. Polarization curves for 304 austenic stainless steel in solutions containing: (a) 1.1 (1.5), (b) 0.55 (1.7), and (c) 0.275 (2.0) M Cl^-, dE/dt 1mV s^{-1} at temperature 25 ^{0}C. The pH solutions in bracket were given.

Figure 2 shows that decrease of Cl^- concentration (curves (a) – (c)) cause a prominent decrease of the cathodic current densities corresponding to hydrogen evaluation reaction [12]:

$$Fe + H^+ = (FeH^+)_{ads} \quad (5)$$
$$(FeH^+)_{ads} \rightarrow (FeH)_{ads} - e^- \quad (6)$$
$$(FeH)_{ads} + H^+ \rightarrow Fe + H_2 - e^-. \quad (7)$$

At more anodic potential an active dissolution region is recorded which is characterized by an anodic current peak that depends on the pH solution (Fig. 2), and decrease with decrease of Cl^- concentration. The formation of peaks concern to passivation of surface steel. The passivation process followed by the produce of thicker oxide film according to the following sequence [28]:

$$Fe + H^+ + ½\, O_2 = (FeOH^-)_{ads} \quad (8)$$
$$(FeOH^-)_{ads} = (FeOH)_{ads} + e^- \quad (8a)$$
$$(FeOH)_{ads} + H^+ + ½\, O_2 = Fe(OH)_2 + 3\, e^- \quad (8b)$$
$$Fe(OH)_2 + H^+ + ½\, O_2 \rightarrow FeOOH + H_2O + 2\, e^-, \quad (8c)$$

or:

$$2\, FeOOH \rightarrow Fe_2O_3 + H_2O. \quad (9)$$

Moreover, formation passive layer can be enriched as a result of following oxides:

$$2\, Cr + 2\, H^+ + 2\, O_2 \rightarrow Cr_2O_3 + H_2O + 14\, e^- \quad (10)$$
$$Ni + 2\, H^+ + O_2 \rightarrow NiO + H_2O + 6\, e^-. \quad (11)$$

The increase of the peak current density with increase in the Cl^- concentration can be explained by the adsorption tendency of the Cl^- ion on the steel surface according to:

$$Fe + Cl^- = (FeCl^-)_{ads} \quad (12)$$
$$(FeCl^-)_{ads} = (FeCl)_{ads} + e^-, \quad (13)$$

similarly form of $(CrCl)_{ads}$ and $(NiCl)_{ads}$.

However, at more anodic potential increase anodic current density because dissolves the passive layer on the surface electrode. In presence of Cl^- the local corrosion would occur according to the following reactions:

$$(FeCl)_{ads} \rightarrow (FeCl^+) + e^- \quad (14)$$
$$(FeCl^+) = Fe^{2+} + Cl^-, \quad (15)$$

similarly form of Cr^{3+} and Ni^{2+} ions.

This means that a passive film on stainless steel is formed even in the acid medium which is a poor electroconductor for which formation and thickening were mainly caused by ionic conductance [32]. The similar considerations relating to corrosion of steel occur in articles [33-35]. The next investigations as corrosive environment were applied solutions which contained 1.1 M Cl^- ions (pH 1.5).

3.1.2. Inhibited solutions

The potentiodynamic polarization curves of 304 austenic stainless steel in corrosive solution in the absence and presence of adenine are shown in Figure 3.

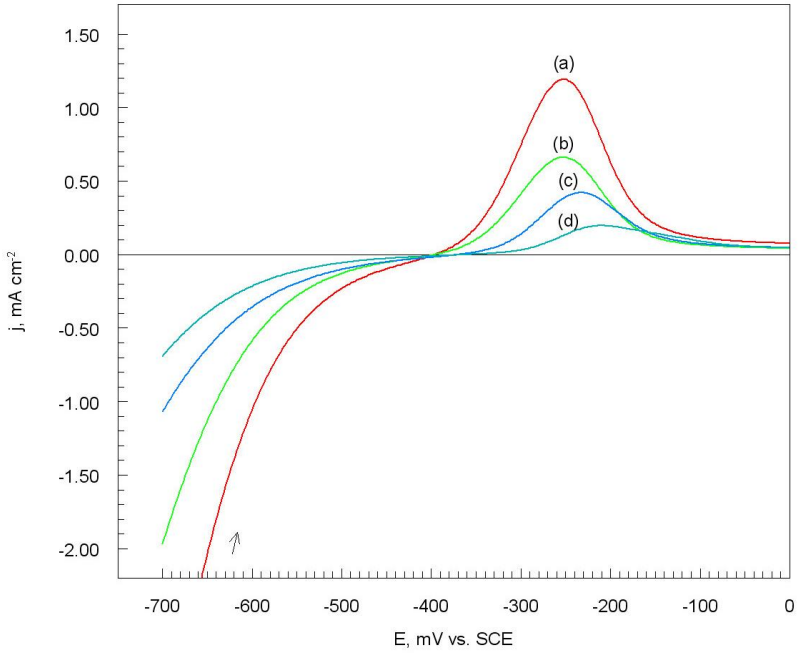

Figure 3. Chosen polarization curves for 304 austenic stainless steel in 1.1 M Cl^- containing different concentrations of adenine: (a) 0, (b) 0.1, (c) 1, and (d) 10 mM, dE/dt 1mV s^{-1} at temperature 25 ^{0}C

Table 1. Corrosion parameters, polarization resistance, degree of surface coverage, and corrosion inhibition efficiency for 304 austenic stainless steel in 1.1 M Cl^- at different concentrations of adenine at temperature 25 ^{0}C

Concentration AD mM	E_{corr} mV vs. SCE	$-b_c$ mV dec^{-1}	b_a mV dec^{-1}	j_{corr} mA cm^{-2}	R_p Ω cm^2	Θ	IE %
0	-396	145	75	0.046	467	---	---
0.1	-396	150	80	0.030	755	0.348	35
0.5	-382	160	80	0.024	965	0.478	48
1	-368	185	80	0.020	1213	0.565	57
5	-362	170	80	0.014	1687	0.696	70
10	-355	160	80	0.007	3262	0.846	85

It could be observed that both the cathodic and anodic reactions were suppressed with the addition of adenine which suggested that the AD reduced the hydrogen evaluation (reactions (5) – (7)) and also retarded anodic dissolution of stainless steel (reactions (8) - (15)). The decrease peak current

density with increase in the adenine concentration can be explained by the adsorption tendency of the AD on the electrode surface. The layer of adenine causes the slow down the reactions of corrosion of steel.

The corrosion parameters i.e. corrosion potential (E_{corr}), cathodic and anodic Tafel slopes (b_c) and (b_a), and corrosion current density (j_{corr}) were obtained from the Tafel extrapolation of the potentiodynamic polarization curves [1,12,24-28], and were given in Table 1.

It should be noted that E_{corr} shifted imperceptibly (about 40 mV) towards more positive values with an increase in the concentration of adenine. The positive shifts of corrosion potential was due to the more effective action exerted on the anodic rather than on the cathodic reaction. Moreover, a increase cathodic (b_c) and invariable anodic (b_a) Tafel slopes indicated only cathodic effect of the inhibition on the corrosion mechanism. The corrosion current density (j_{corr}) decreased when the concentration of adenine was increased (Table 1) which indicates the inhibiting effect of AD. The polarization resistance values (R_p) for 304 austenic stainless steel (which were calculated by Equation (1)) increased with an increase in the concentration of an inhibitor (Table 1). The surface of electrode was covered by layer of adenine making difficult the exchange the charge with depth of electrolyte. However, the degree of surface coverage was calculated on basis the Equation (2). The results showed an increase in the degree of surface electrode by adsorption of adenine on steel surface. Consequently, the corrosion inhibition efficiency can also be calculated from polarization tests by using the Equation (3). The values *IE* are presented in Table 1. It is clear that in the presence of AD the inhibition efficiency increases with an increase in the concentration of inhibitor.

3.2. Corrosion rate

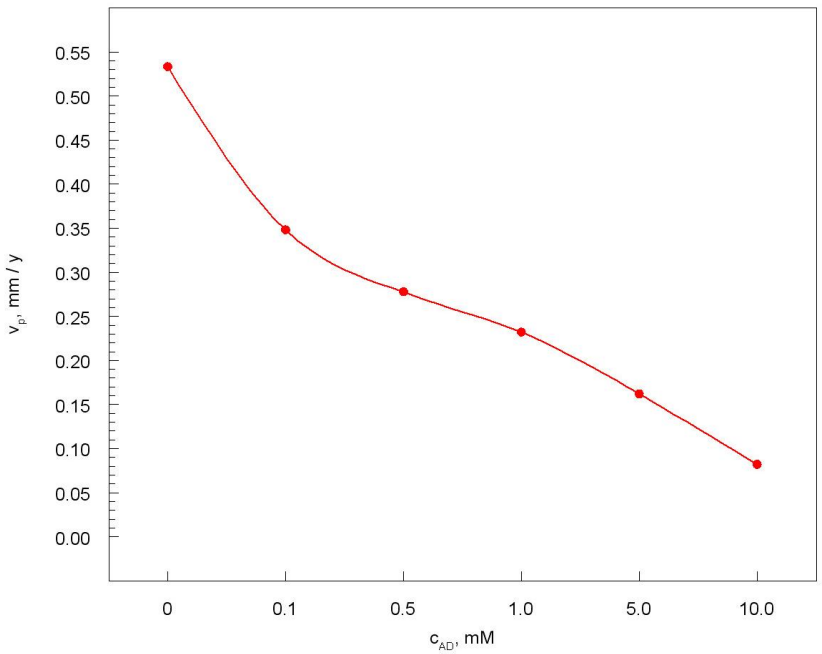

Figure 4. Relationship between corrosion rate of 304 austenic stainless steel and of adenine concentration in the presence of 1.1 M Cl^- at temperature 25 ^{0}C

The corrosion current density (Table 1) was converted into the corrosion rate (υ_p) of stainless steel by using the Equation (4) [28,31]. The values of 304 austenic stainless steel corrosion rate in the absence and presence of adenine are shown in Figure 4.

The corrosion rate of stainless steel is significantly reduced as a result of the reduction in the j_{corr}. The υ_p of stainless steel in 1.1 M Cl^- solution without inhibitor is found to be 0.533 mm/year which is ~7 times lower in solution with 10 mM of AD. This result reveals the capability of adenine to act as a corrosion protective layer on 304 austenic stainless steel surface.

3.3. Activation parameters of the corrosion process

The effect of temperature (in range 30 – 60 ^{0}C) on the 304 austenic stainless steel general corrosion inhibition by adenine was studied. Figure 5 shows Tafel polarization plots recorded for investigated steel in presence 10 mM of adenine at various temperatures. The similar curves were recorded for another concentrations of inhibitor.

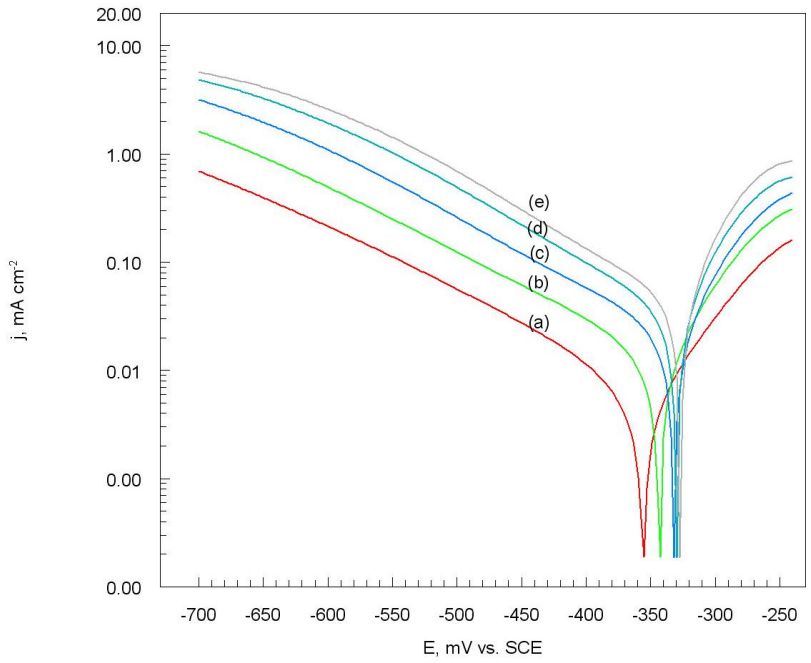

Figure 5. Tafel polarization plots for 304 austenic stainless steel in 1.1 M Cl^- containing 10 mM of adenine at various temperatures: (a) 25, (b) 30, (c) 40, (d) 50, and (f) 60 ^{0}C, dE/dt 1mV s^{-1}

The chosen values of the corrosion parameters (obtained from the Tafel extrapolation of the polarization curves) the degree of surface coverage, and corrosion inhibition efficiency at various concentrations of adenine at all studied temperatures are depicted in Table 2.

The addition of adenine shifts a bit (~40 mV) the corrosion potential towards the positive values independently than temperature of solution. It may be concluded that of AD should be considered as a mixed-type inhibitor, meaning that the addition of adenine to 1.1 M Cl^- solution both

reduces the anodic dissolution of 304 austenic stainless steel, and also retards the cathodic hydrogen evolution reaction. For the same values concentration of inhibitor an increase in temperature increases corrosion current density. However, addition of AD cause decreases the j_{corr} values across the temperature range. The results also indicate that the inhibition efficiency increase with the increase of concentration of adenine and temperature of solution (Table 2). Such behaviour can be interpreted that the inhibitor acts by adsorbing onto the metal surface, and strongly joins with surface of steel probably. Nevertheless, the adsorption of an organic molecule is not considered as a purely physical or chemical adsorption phenomenon. A wide spectrum of conditions, ranging from the dominance of chemisorptions or electrostatic effects, arises from other experimental data on adsorption.

Table 2. Chosen corrosion parameters, degree of surface coverage, and corrosion inhibition efficiency for 304 austenic stainless steel in 1.1 M Cl^- with different concentrations of adenine at various temperatures

Temperature ^0C	Concentration AD mM	E_{corr} mV vs. SCE	j_{corr} mA cm^{-2}	Θ	IE %
30	0	-387	0.079	---	---
	0.1	-387	0.050	0.367	37
	0.5	-374	0.040	0.494	49
	1	-361	0.031	0.608	61
	5	-352	0.021	0.734	73
	10	-342	0.010	0.873	87
40	0	-370	0.200	---	---
	0.1	-370	0.120	0.400	40
	0.5	-359	0.085	0.575	58
	1	-349	0.050	0.750	75
	5	-341	0.036	0.820	82
	10	-332	0.022	0.890	89
50	0	-370	0.420	---	---
	0.1	-370	0.210	0.500	50
	0.5	-358	0.150	0.643	64
	1	-345	0.085	0.798	80
	5	-337	0.059	0.859	86
	10	-329	0.032	0.924	92
60	0	-370	0.650	---	---
	0.1	-370	0.300	0.538	54
	0.5	-355	0.260	0.600	60
	1	-340	0.125	0.808	81
	5	-333	0.083	0.872	87
	10	-325	0.041	0.937	94

The activation parameters such as: the activation of energy (E_a) the enthalpy of activation (ΔH_a) and the entropy of activation (ΔS_a) in the range of studied temperatures (30 – 60 ^{0}C) for both corrosion and corrosion inhibition of 304 austenic stainless steel in 1.1 M Cl^- in the absence and presence of various concentrations of adenine were calculated from Arrhenius – type plot [28,36,37]:

$$j_{corr} = A\,exp\left(\frac{-E_a}{R\,T}\right) \quad (16)$$

and transition – state equation:

$$j_{corr} = \left(\frac{R\,T}{N\,h}\right) exp\left(\frac{\Delta S_a}{R}\right) exp\left(\frac{-\Delta H_a}{R\,T}\right) \quad (17)$$

where A is the Arrhenius constant, E_a is the apparent activation energy, N is the Avogadro's constant, h is the Planck's constant, ΔS_a is the change of entropy for activation, ΔH_a is the change of enthalpy for activation.

The plots of ln (j_{corr}) vs. 1/T, Figure 6 and ln (j_{corr}/T) vs. 1/T, Figure 7 give straight lines with slopes of $-E_a/R$ and $-\Delta H_a/R$ respectively. The intercepts which can them be calculated, will be ln (A) and [ln ($R/N\,h$) + ($\Delta S_a/R$)] for the Arrhenius and transition-state equations, respectively.

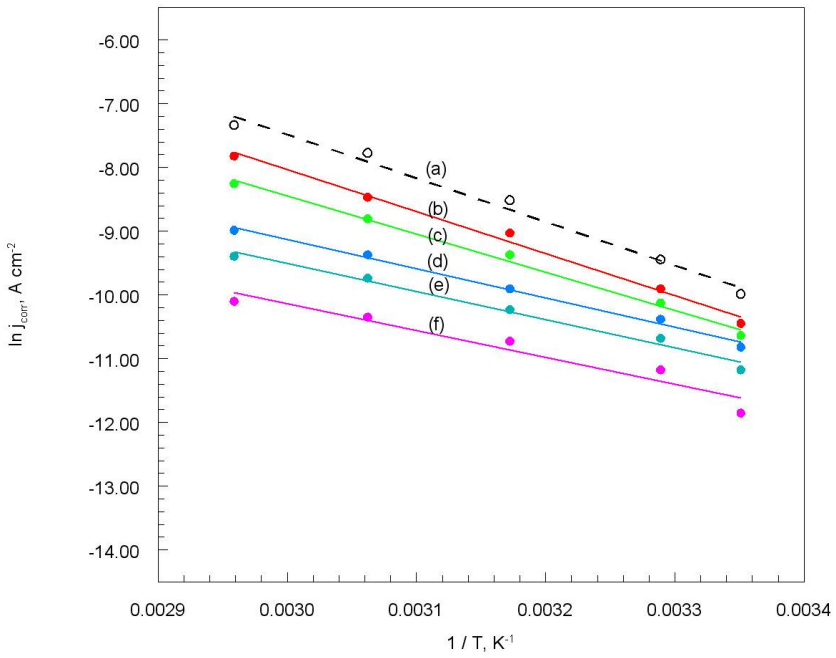

Figure 6. Arrhenius plots for 304 austenic stainless steel in 1.1 M Cl^- containing different concentrations of adenine: (a) 0, (b) 0.1, (c) 0.5, (d) 1, (e) 5, and (f) 10 mM

The calculated values of E_a, ΔH_a and ΔS_a are summarized in Table 3. In the presence increasing of adenine concentration the decrease of E_a values were observed. The decrease in apparent activation energy arises from a shift of the net corrosion reaction, from one on the uncovered surface to one directly involving the adsorbed sites [38]. The values E_a and ΔH_a are nearly the same (Table 3) and are smaller in the presence of adenine than in a blank solution, indicating that the energy barrier of the

corrosion reaction decreased in the presence of inhibitor without changing the mechanism of dissolution of metal. The entropy of activation, ΔS_a in the absence and presence of adenine are negative, implying that the rate-determining step for the activated complex is the association rather than the dissociation step.

In the presence of the inhibitor, ΔS_a moves in direction of negative values (Table 3), which implies that the adsorption process is accompanied by an decrease in entropy, which is the driving force for the adsorption of adenine onto the austenic stainless steel surface.

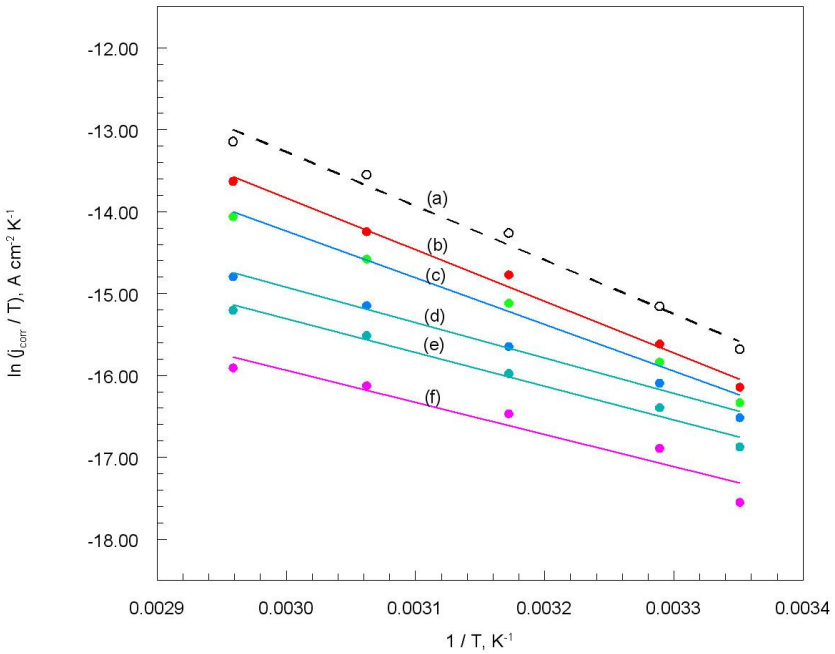

Figure 7. Transition state plots for 304 austenic stainless steel in 1.1 M Cl^- containing different concentrations of adenine: (a) 0, (b) 0.1, (c) 0.5, (d) 1, (e) 5, and (f) 10 mM

Table 3. Corrosion kinetic parameters for 304 austenic stainless steel in 1.1 M Cl^- at different concentrations of adenine

Concentration AD mM	E_a kJ mol^{-1}	ΔH_a kJ mol^{-1}	ΔS_a J mol^{-1} K^{-1}
0	63.37	60.75	-123.16
0.1	60.73	58.12	-135.91
0.5	55.30	52.69	-155.76
1	42.42	39.80	-200.63
5	40.70	38.09	-209.03
10	38.75	36.13	-220.22

3.4. Thermodynamic parameters of the adsorption isotherm

The efficiency of organic molecules as good corrosion inhibitors depends mainly on their adsorption ability on the metal surface. Basic information about the interaction between inhibitor and metal can be provided by the adsorption isotherm. The investigation of the relation between corrosion inhibition and adsorption of inhibitor is of great importance.

The surface coverage (Tables 1 and 2) and the concentration of adenine solution (c_{AD}) were tested by fitting to various isotherms like: Langmuir, Temkin and Freundlich. However, the best fit was obtained with Langmuir isotherm as shown in Figure 8 which is given by following equation [28]:

$$\frac{c_{AD}}{\Theta} = \frac{1}{K_{ads}} + c_{AD} \qquad (18)$$

where K_{ads} is the equilibrium constant of the adsorption/desorption processes, and it reflects the affinity of the inhibitor molecules towards surface adsorption sites.

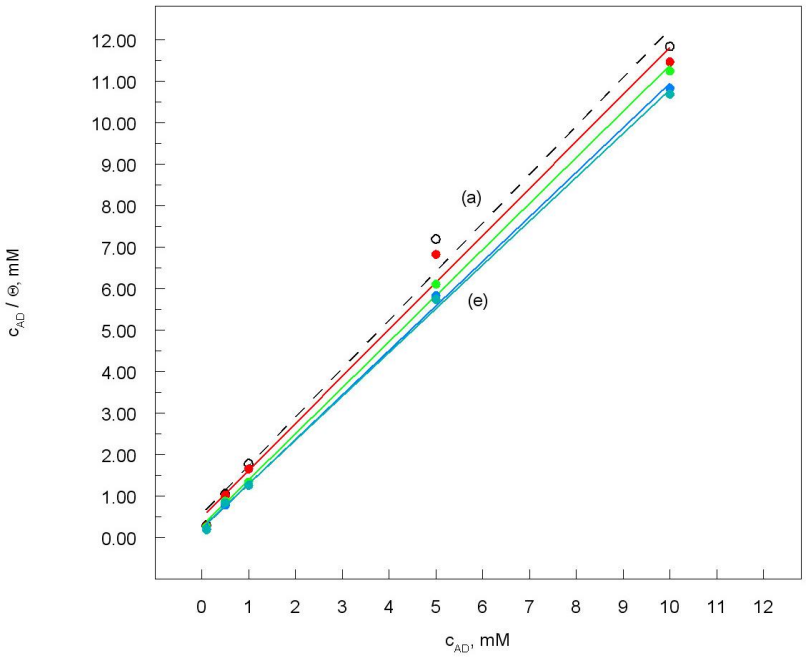

Figure 8. Langmuir adsorption plots of adenine onto the 304 austenic stainless steel in 1.1 M Cl^- at various temperatures: (a) 25, (b) 30, (c) 40, (d) 50, and (e) 60 ^{0}C

Though, the plots of c_{AD}/Θ vs. c_{AD} (Fig. 8) were linear (correlation 0.996 – 0.999) the deviation of the slopes from unity at the studied temperatures for ideal Langmuir adsorption isotherm. From the intercepts of the straight lines on the $c_{AD}/0$ axis (Fig. 8) leads to values equilibrium constant for the adsorption/desorption of adenine process Table 4. The high value of K_{ads} reveals that the AD molecule possesses strong adsorption ability onto the 304 austenic stainless steel.

However, the K_{ads} increased with an increase of temperature indicating that adsorption of adenine onto the metal surface was favorable at higher temperature.

The equilibrium constant of the adsorption/desorption (K_{ads}) were related to the standard free energy of adsorption according to equation [28,31,37,38]:

$$\Delta G^{0}_{ads} = - RT \ln (55.5\, K_{ads}) \quad (19)$$

where R is the universal gas constant, T is the absolute temperature, and value 55.5 is concentration of water in solutions.

Table 4. Equilibrium constant adsorption/desorption and standard free: energy, enthalpy, and entropy of the adsorption onto the 304 austenic stainless steel in 1.1 M Cl^- solution in the presence of adenine at various temperatures

Temperature ^{0}C	K_{ads} mol^{-1}	ΔG^0_{ads} kJ mol^{-1}	ΔH^0_{ads} kJ mol^{-1}	ΔS^0_{ads} J mol^{-1}K^{-1}
25	1.83×10^3	-28.57		168.15
30	2.05×10^3	-28.85		169.09
40	3.66×10^3	-30.28	21.54	173.89
50	3.95×10^3	-30.47		174.53
60	4.31×10^3	-30.69		175.27

The standard free energy of adsorption were calculated and are given in Table 4.Generally the standard free energy of adsorption values of -20 kJ mol^{-1} or less negative are associated with an electrostatic interaction between charged metal surface (physical adsorption), those of -40 kJ mol^{-1} or more negative involves charge sharing or transfer from the inhibitor molecules to the metal surface to form a co-ordinate covalent bond (chemical adsorption) [39,40].

The values of standard free energy of adsorption of adenine onto the 304 austenic stainless steel surface were found as -28.57 and -30.69 kJ mol^{-1} at temperatures 25 and 60 ^{0}C respectively (Table 4). Therefore, it can be concluded that the adsorption of adenine onto the steel surface takes place through both physical and chemical adsorption, namely mixed type with predominant chemical one [41-43].

The Langmuir isotherm assumes that the 304 austenic stainless steel surface contains a fixed number of adsorption sites, and each site holds one molecule of adenine (adsorbate). One adsorbed H_2O molecule is replaced by one of AD molecule on the metal surface:

$$AD_{(sol)} + H_2O_{(ads)} \leftrightarrow AD_{(ads)} + H_2O_{(sol)}, \quad (20)$$

moreover, the adsorption of adenine molecule onto the 304 austenic stainless steel is monolayer. The strong interaction and stability of the adsorbed layer with stainless surface. The adsorption of adenine

on the electrode surface makes a barrier for mass and charge transfers. This situation leads to the protection of austenic stainless steel surface from the attack of aggressive forms of solution.

Voluble information about the mechanism of corrosion inhibition can be provided by the values of thermodynamic parameters for the adsorption of inhibitor. Thermodynamically, ΔG^0_{ads} were related to the standard enthalpy, ΔH^0_{ads} and standard entropy, ΔS^0_{ads} according to [28,35,37]:

$$\Delta G^0_{ads} = \Delta H^0_{ads} - T\,\Delta S^0_{ads} \quad (21)$$

and the standard enthalpy of adsorption can be calculated on basis the Van't Hoff formula:

$$ln\ K_{ads} = \frac{-\Delta H^0_{ads}}{R\,T} + const. \quad (22)$$

or:

$$log\ K_{ads} = \frac{-\Delta H^0_{ads}}{2.303\,RT} + \frac{\Delta S^0_{ads}}{2.303\,RT} \quad (22a)$$

A plot of ln K_{ads} vs. 1/T gives a straight line, as shown in Figure 9. The slope of the straight line $-\Delta H^0_{ads}/R$.

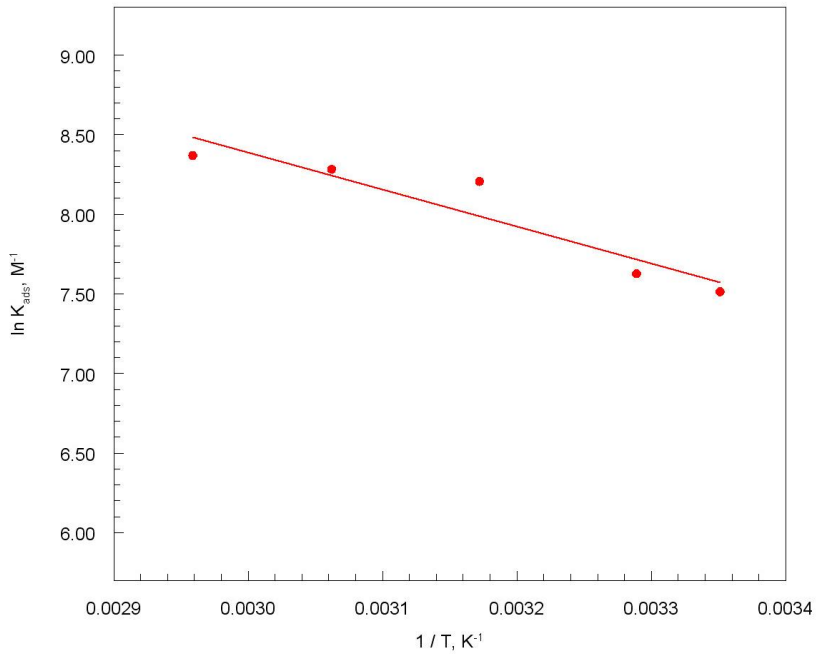

Figure 9. Van't Hoff plot for 304 austenic stainless steel in 1.1 M Cl^- containing of adenine

The value of standard enthalpy adsorption is given in Table 4. Since the ΔH^0_{ads} value is positive the adsorption of adenine molecules onto the 304 austenic stainless steel surface is an endothermic process which indicates that inhibition efficiencies (Table 2) increase with the increase of temperature. Such behaviour can be interpreted that increasing temperature does not cause desorption of adenine molecules from the metal surface.

The standard entropy adsorption, ΔS^0_{ads} of inhibitor can be calculated from Equation (21) according to [28]:

$$\Delta S^0_{ads} = \frac{\Delta H^0_{ads} - \Delta G^0_{ads}}{T} \quad (23)$$

The calculated values of ΔS^0_{ads} are recorded in Table 4. It is obvious that the values of standard entropy adsorption are positive. The positive sign of ΔS^0_{ads} arise from substitution process (20) which can be attributed to the increase in the solvent entropy and more positive water desorption entropy [44]. It also means that increasing in disordering takes place is going from reactants to the metal/solution interface [45] which is the driving force for the adsorption of adenine onto the 304 austenic stainless steel surface.

3.5. Quantum chemical study

To investigate the correlation between molecular structure of adenine and its inhibition effect, quantum chemical parameters has been performed.

Protection efficiency of inhibitors depends on the electronic properties of the corrosion inhibitors such as: highest occupied molecular orbital (HOMO), the lowest unoccupied molecular orbital (LUMO).

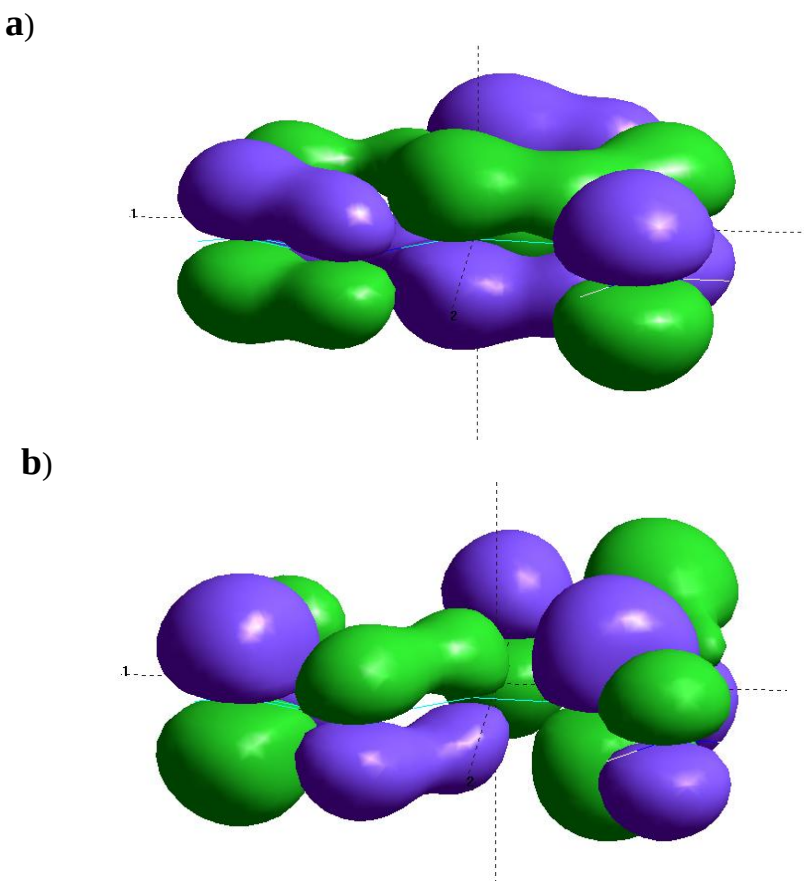

Figure 10. The frontier molecular orbital density distribution for adenine: a) HOMO, b) LUMO

It has been reported [46-48] that the higher the HOMO energy of the inhibitor the greater the trend of offering electrons to unoccupied *d* orbital of the metal, and the higher the corrosion efficiency. In addition, the lower the LUMO energy the easier the acceptance of electrons from metal surface. The frontier molecular orbital density distributions of HOMO and LUMO for adenine were shown in Figure 10.

Table 5. The calculated quantum chemical parameters for adenine

Inhibitor	E_{HOMO} eV	E_{LUMO} eV	ΔE eV	μ D	I eV	A eV	χ eV	η eV	ΔN
AD	-8.556	-0.234	-8.322	2.200	8.556	0.234	4.395	4.161	0.313

The relevant quantum chemical parameters for adenine were listed in Table 5.

The higher value of E_{HOMO} suggests that the adenine molecule offering electrons to unoccupied *d* orbital of the metal, while the higher value of the $\Delta E = E_{LUMO} - E_{HOMO}$ proves about the more stable molecule of adenine.

Remaining quantities (Table 5) are related to ionization potential, $I = -E_{HOMO}$, and electron affinity, $A = -E_{LUMO}$ of the studied molecule. The obtained values of I and A were considered for the calculation of the electronegativity, χ and the global hardness, η using the following relations:

$$\chi = \frac{I + A}{2} \quad (24)$$

and:

$$\eta = \frac{I - A}{2} \quad (25)$$

The calculated parameters are listed in Table 5.

The fraction of electrons transferred from the adenine molecule to the iron atom, ΔN was calculated according to Person's formula:

$$\Delta N = \frac{\chi_{Fe} - \chi_{PU}}{2(\eta_{Fe} + \eta_{PU})} \quad (26)$$

The idea behind this is that in the reaction of two systems with different electronegativity as a metallic surface and an inhibitor molecule, the following mechanism will take place: the electron flow will move from the molecule with the low electronegativity towards that of a higher value until the chemical potentials are the same.

The theoretical values of χ_{Fe} and η_{Fe} are 7.0 and 0 eV mol^{-1}, respectively [49,50]. The fraction of electrons transferred (ΔN) from adenine to the iron molecule was calculated (Table 5). The value of ΔN showed inhibition effect of AD resulted from electron donation. The adenine was the donators of electrons while the stainless steel was acceptor. However, atoms of nitrogen (Fig. 1) have the most probability to form coordinating bond, while the other electronegative atoms (for example *C*) cannot combine with metal surface with regard on the steric effects. The adenine was bound to the 304 austenic stainless steel surface and thus formed inhibition adsorption layer against corrosion.

3.6. Scanning electron microscopy studies

The Figure 11 show the surface morphology of 304 austenic stainless steel specimens in the a) absence, and b) in the presence of adenine. The Figure 11a) revels that the surface was strongly damaged in absence of the inhibitor. Chloride ions, oxygen and water penetrate the surface through pores, flaws or other weak spots what results in the further corrosion of investigated steel. There are wide and deep pits on the surface which indicate the main characteristic of pitting corrosion.

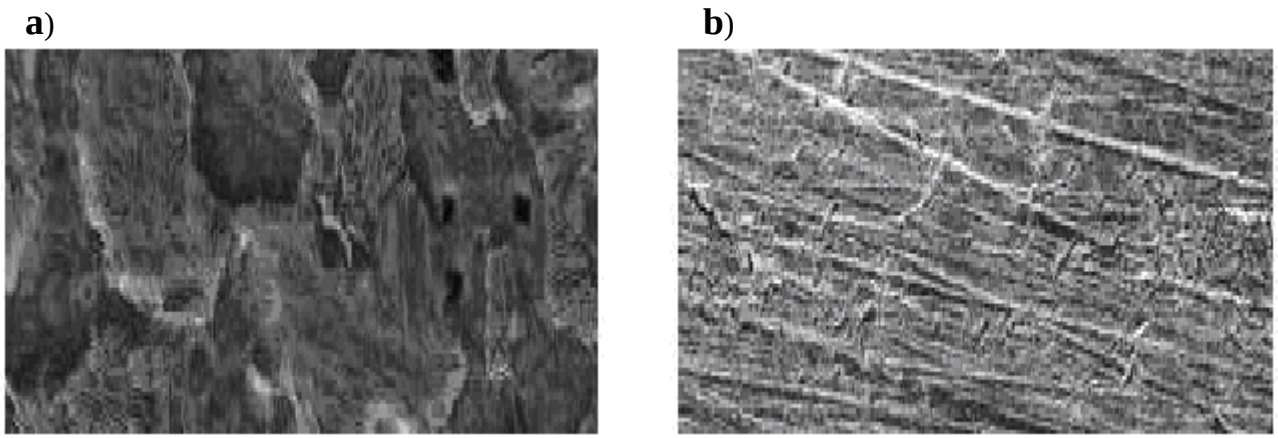

Figure 11. SEM micrographs of 304 austenic stainless steel surface after expose 360 hours to 1.1 M Cl^- solution: a) without, b) with the addition of 10 mM adenine. Magnification 800×

The Figure 11b) shows SEM image of 304 austenic stainless steel surface after immersion (for the same time interval) in corrosive solution containing additionally 10 mM of adenine. The surface of steel is more uniform in the inhibited solution than the surface in the absence of adenine except some hallows structures which most probably due to polishing lines. The image clearly demonstrate the high corrosion inhibition efficiency of AD in aggressive chloride solution. The inhibitor molecules were adsorbed on the active sites and protected the austenic stainless steel against corrosion.

4. MECHANISM OF INHIBITION

The corrosion inhibition mechanism in acid medium the most often depends on the adsorption of an inhibitor onto the metal surface. The inhibitive action of inhibitors depends on the electron densities around the adsorption centers. The higher the electron density at the centre, the more efficient is the inhibitor.

The adsorption of the inhibitor on metal surface is the first step in the action mechanism of inhibition. Physical adsorption requires presence of both electrically charged surface of the metal and charged species in the bulk of the solution. Moreover, chemical adsorption requires in the presence of

a metal to have a vacant low-energy electron orbital, and an inhibitor with molecules having relatively loosely bond electrons or heteroatom with lone pair electrons.

Therefore, it may be assumed that adenine adsorption can also occur via electrostatic interaction with the surface of the loaded electrode: positively across atoms: *N* (+0.166), and *N* (+0.279) or negatively across *N* (-0.069), *N* (-0.173), and *N* (-0.262) (Fig. 1).

Moreover, in this case the insoluble film consisting from: $(FeCl)_{ads}$, $(CrCl)_{ads}$ and $(NiCl)_{ads}$ precipitates upon the surface of the stainless steel electrode (reactions (12) – (13)). They act as a protective barrier safeguarding steel from further oxidation. The action of Cl^- can be physically interpreted as blockage of the steel surface. Unfortunately, the insoluble film was leaky on the electrode surface. In aqueous acid solutions of adenine can exist as cationic species [24-27]:

$$AD + H^+ \leftrightarrow ADH^+. \quad (27)$$

However, in presence of adenine a protective layer has been formed according reaction:

$$(Fe-Cl)_{ads} + ADH^+ \leftrightarrow (Fe-AD)_{ads} + H^+ + Cl^-, \quad (28)$$

similarly form protective layers: $(Cr-AD)_{ads}$, and $(Ni-AD)_{ads}$.

The inhibiting effect of adenine can be regarded as an adsorption inhibitor and the formation compound protective film onto of 304 austenic stainless steel surface. The adsorption film of adenine makes a barrier for mass and charge transfers. This situation leads to the protection of the austenic stainless steel surface from the attack of aggressive anions of the chloride acid solution.

5. CONCLUSION

The inhibition effect of adenine on the corrosion of 304 austenic stainless steel in chloride acid solutions was studied. From the data obtained the following points can be emphasized:

(1) The adenine has good inhibition effect for the corrosion of 304 austenic stainless steel in 1.1 M Cl^- acid solution, and inhibition efficiency was increased with inhibitor concentration.

(2) The of adenine behaves rather as mixed type corrosion inhibitor of steel by inhibiting both cathodic hydrogen evolution and anodic metal dissolution reactions.

(3) The values of E_a and ΔH_a indicate that the energy barrier of the corrosion reaction decreased in the presence of adenine without changing the mechanism of dissolution of steel. The negative values of ΔS_a implying that the rate-determining step for the activated complex is the association rather than the dissociation step.

(4) The Langmuir adsorption isotherm exhibited the best fit to the experimental data. The values of adsorption equilibrium constant suggested that of AD strongly adsorbed on the surface, forming a protective film.

(5) The corrosion inhibition efficiency of investigated stainless steel increased with temperature for the same concentration of adenine.

(6) The negative sign of ΔG^0_{ads} and positive of ΔH^0_{ads} indicate that the adsorption process of AD is spontaneous and endothermic. The positive of ΔS^0_{ads} can be attributed to the increase in the solvent entropy and more positive water desorption entropy.

(7) The quantum chemical method shows that of adenine molecules can be directly adsorbed at the steel surface on the basis of donor-acceptor interactions between the π-electrons of benzene ring, and *N* atoms, or the vacant *d*-orbital of metal atoms.

(8) The SEM micrographs showed that the inhibitor molecules form a good protective film onto the 304 austenic stainless steel surface.

ACKNOWLEDGMENTS
This work was supported by the ESF Human Capital Operational Programme grant 6/1/8.2.1./POKL/ 2009.

References

1. F. Jr. Depenyou, A. Doubl, S. Laminsi, D. Moussa, J.L. Brisset, J.-M. Le Breton, *Corros. Sci.* 50 (2008) 1422
2. C.O.A. Olsson, D. Landolt, *Electrochim. Acta* 48 (2003) 1093
3. S. Bera, S. Rangarajan, S.V. Narasimhan, *Corros. Sci.* 42 (2000) 1709
4. L.V. Taveira, G. Frank, H.P. Strunk, L.F.P. Dick, *Corros. Sci.* 47 (2005) 757
5. F. Deflorian, S. Rossi, *Electrochim. Acta* 51 (2006) 1736
6. E. Gracia-Ochoa, J. Genesca, *Surf. Coat. Tech.* 184 (2004) 322
7. W.H. Li, Q. He, S.T. Zhang, C.L. Pei, B.R. Hou, *J. Appl. Electrochem.* 38 (2008) 289
8. P. Morales-Gil, G. Negrón-Siliva, M. Romero-Romoa, *Electrochim. Acta* 49 (2004) 4733
9. M. Lashkari, M.R. Arshadi, *Chem. Phys.* 299 (2004) 131
10. M. Bouklah, A. Oussini, B. Hammouti, A. El-Idrissi, *Appl. Surf. Sci.* 250 (2005) 50
11. M.A. Veloz, I.G. Martinez, *Corrosion* 62 (2006) 283
12. M. Abdallah, *Mater. Chem. Phys.* 82 (2003) 786
13. A. Ouchrif, M. Zegmout, B. Hammouti, S. El-Kadiri, A. Ramdani, *Appl. Surf. Sci.* 252 (2005) 339
14. S.A. Abd El-Maksoud, *Appl. Surf. Sci.* 206 (2003) 129
15. A. Chetouani, A. Aouniti, B. Hammouti, N. Benchat, T. Benhadda, S. Kertit, *Corros. Sci.* 45 (2003) 1675
16. A.A. Ismail, S.H. Sand, A.A. El-Meligi, *J. Mater. Sci. Technol.* 16 (2000) 397
17. M. Düdükcü, B. Yazici, M. Erbil, *Mater. Chem. Phys.* 87 (2004) 138
18. L.B. Tang, X.M. Li, Y.S. Si, G.N. Mu, G.H. Liu, *Mater. Chem. Phys.* 95 (2006) 29
19. A.A. Aksüt, S. Bilgiç, *Corros. Sci.* 33 (1992) 379
20. S. Bilgiç, A.A. Aksüt, *Br. Corros. J.* 28 (1993) 59
21. S. Martinez, I. Štern, *Chem. Biochem. Eng. Quart.* 13 (1999) 191
22. G. Moretti, F. Guidi, *Corros. Sci.* 44 (2002) 1995
23. G. Quartarone, T. Bellomi, A. Zingales, *Corros. Sci.* 45 (2003) 715
24. M. Scendo, *Corros. Sci.* 49 (2007) 373
25. M. Scendo, *Corros. Sci.* 49 (2007) 2985
26. M. Scendo, *Corros. Sci.* 49 (2007) 3953
27. M. Scendo, *Corros. Sci.* 50 (2008) 1584
28. M. Scendo, N. Radek, J. Trela, *Corros. Rev.* 30 (2012) 33

29. A.R. Katritzky, Comprehensive Heterocyclic Chemistry. *The Structure, Reaction, Synthesis and Uses of Heterocyclic Compounds*, vol. 5, Pergamon Press Ltd., London, 1984
30. M.K. Pavithra, T.V. Venkatesha, K. Vathsala, K.O. Nayana, *Corros. Sci.* 52 (2010) 3811
31. M.A. Amin, M.M. Ibrahim, *Corros. Sci.* 53 (2011) 873
32. M.S.S. Morad, A.A.A. Hermas, *J. Chem. Technol. Biotechnol.* 76 (2001) 401
33. Q. Hu, G. Zhang, Y. Qiu, X. Guo, *Corros. Sci.* 53 (2011) 4065
34. El-Sayed, M. Sherif, *Mat. Chem. Phys.* 129 (2011) 961
35. S.E. Nataraja, T.V. Venkatesha, H.C. Tandon, *Corros. Sci.* 60 (2012) 214
36. G.E. Badr, *Corros. Sci.* 51 (2009) 2629
37. F. El-Taib Heakal, A.S. Fouda, M.S. Radwan, *Mater. Chem. Phys.* 125 (2011) 26
38. X. Li, S. Deng, H. Fu, G. Mu, *Corros. Sci.* 50 (2008) 2635
39. X. Wang, H. Yang, F. Wang, *Corros. Sci.* 53 (2011) 113
40. N.O. Obi-Egbedi, I.B. Obot, *Corros. Sci.* 53 (2011) 263
41. I. Ahamad, R. Prasad, M.A. Quraishi, *Corros. Sci.* 52 (2010) 3033
42. X. Li, S. Deng, H. Fu, *Corros. Sci.* 53 (2011) 302
43. S. Deng, X. Li, H. Fu, *Corros. Sci.* 53 (2011) 822
44. X. Li, S. Deng, H. Fu, G. Mu, *Corros. Sci.* 47 (2005) 1932
45. G. Mu, X. Li, G. Liu, *Corros. Sci.* 47 (2005) 1932
46. S. Ramachandran, B.L. Tsai, M. Blanco, H. Chen, Y. Tang, W.A. Goddard, *J. Phys. Chem.* A 101 (1997) 83
47. I. Lukovits I, K. Palfi, E. Kalman, *Corrosion* 53 (1997) 915
48. E.H. El-Ashri, A. El-Nemr, S.A. Essawy, S. Ragub, *Electrochim. Acta* 51 (2006) 3957
49. H. Ju, Z. Kai, Y. Li, *Corros. Sci.* 50 (2008) 865
50. A.Y. Musa, A.A.H. Kadhum, A.B. Mohamad, A.A.B. Rahoma, H. Mesmari, *J. Mol. Struct.* 969 (2010) 233